

To appear in *Physical Review B***Charge-Stripe Ordering From Local Octahedral Tilts: Underdoped and Superconducting $\text{La}_{2-x}\text{Sr}_x\text{CuO}_4$ ($0 \leq x \leq 0.30$)**

E. S. Božin, S. J. L. Billinge,

*Department of Physics and Astronomy and Center for Fundamental Materials Research,
Michigan State University, East Lansing, MI 48824-1116.*

G. H. Kwei,

Los Alamos National Laboratory, Los Alamos, NM 87545.

H. Takagi

Institute for Solid State Physics, University of Tokyo, 7-22-1, Roppongi, Minato-ku, Tokyo, 106, JAPAN

(November 7, 2018)

The local structure of $\text{La}_{2-x}\text{Sr}_x\text{CuO}_4$, for $0 \leq x \leq 0.30$, has been investigated using the atomic pair distribution function (PDF) analysis of neutron powder diffraction data. The local octahedral tilts are studied to look for evidence of [110] symmetry (i.e., LTT-symmetry) tilts locally, even though the average tilts have [010] symmetry (i.e., LTO-symmetry) in these compounds. We argue that this observation would suggest the presence of local charge-stripe order. We show that the tilts are locally LTO in the undoped phase, in agreement with the average crystal structure. At non-zero doping the PDF data are consistent with the presence of local tilt disorder in the form of a mixture of LTO and LTT local tilt directions and a distribution of local tilt magnitudes. We present topological tilt models which qualitatively explain the origin of tilt disorder in the presence of charge stripes and show that the PDF data are well explained by such a mixture of locally small and large amplitude tilts.

61.12-q,71.38.+i,74.20.Mn,74.72.Dn,74.72.-h

I. INTRODUCTION

There is now considerable experimental evidence for the existence of striped charge distributions in the strongly correlated materials $\text{La}_{2-x}\text{Sr}_x\text{NiO}_{4+\delta}$,¹⁻⁴ $\text{La}_{2-x-y}\text{Nd}_y\text{Sr}_x\text{CuO}_{4+\delta}$,⁵⁻⁷ and $\text{La}_{1-x}\text{Ca}_x\text{MnO}_3$.⁸⁻¹⁰ There is also growing circumstantial evidence that similar striped charge distributions are present more widely in other high-temperature superconducting cuprates,¹¹⁻¹⁴ and their possible importance in producing the high-temperature superconductivity itself is the subject of intensive investigation.¹⁵⁻²⁰ A number of recent reviews describe observations of lattice effects in the high-temperature superconductors in general.²¹⁻²⁶ However, there is currently no direct evidence that these stripe phases exist in superconducting samples, although there has been an observation where stripes and superconductivity were observed in the same samples.²⁷ It is important to show that local charge-stripe ordered domains really exist in the superconducting regions of samples to establish the importance of charge-stripes in the superconducting phenomenon.

A local structural probe is useful for investigating the existence or absence of short-range ordered stripes since it is known that the charge-stripes produce a structural distortion. When the stripes are long-range ordered the structural modulation becomes periodic and

a superlattice is observed in neutron, x-ray and electron diffraction.^{5,6,8,9,27,28} The absence of superlattice peaks can mean that the stripe order has disappeared. However, it is also possible that the stripes persist locally but are not long-range ordered and are fluctuating. In this latter case the *local* structural distortion due to the inhomogeneous charge distribution will persist even when the superlattice peaks have disappeared. A probe of local structure can therefore give information about whether local stripe order exists even in the absence of superlattice peaks. In this study we use the atomic pair distribution function (PDF) analysis²⁹⁻³¹ of powder neutron diffraction data to look for evidence of local charge stripe order in $\text{La}_{2-x}\text{Sr}_x\text{CuO}_{4+\delta}$.

An amenable system for this kind of study is the series of compounds based around $\text{La}_{2-x}(\text{Sr},\text{Ba})_x\text{CuO}_4$ (2:1:4 compounds) because in these compounds collective tilts of the CuO_6 octahedra exist which couple strongly to the electronic system³²⁻³⁶ and the charge-stripes.^{5,6} In particular, it has been observed that long-range ordered charge-stripes are only seen in the cuprate system when the octahedra tilt collectively about axes along the Cu-O bonds, i.e., in the [110] crystallographic directions in the standard crystallographic setting ($P4_2/\text{ncm}$ for the LTT phase).^{5,6,27} This tilt pattern is the one observed in the low temperature tetragonal (LTT) phase.³⁷ Most of the superconducting compositions are in the alternative low

temperature orthorhombic (LTO) phase³⁸ which has the octahedra tilting *on average* about axes parallel to the [100] crystallographic direction. It is thought that since the charge-stripes lie in [110] directions in the lattice (i.e., along Cu-O bonds), the [100] type LTO tilts prevent the stripes from ordering statically over long range. Because the charge-stripes are strongly coupled to the octahedral tilts,^{5,6} we can use the octahedral tilts as a probe of the local stripe order.

In a previous paper,³⁹ we showed that in $\text{La}_{1.875}\text{Ba}_{0.125}\text{CuO}_4$, local regions of LTT-type octahedral tilt order persist in the LTO phase above the LTO-LTT phase transition. It was suggested that the LTO phase is made up of short-range ordered LTT-domains but that a linear combination of different LTT variants resulted in the average LTO tilt order observed in the crystallographic structure. There also are other observations that the local tilts in 2:1:4 materials are not always the same as those measured crystallographically.^{11,40-44} At the time of the earlier paper,³⁹ charge stripes had not been observed in the cuprates and it was unclear why the LTO phase should be made up of inhomogeneous domains of short-range LTT-order.^{45,46} However, the presence of dynamic charge-stripe domains provides a very natural explanation of this unexpected result.

In the present work we have studied the local octahedral tilts in $\text{La}_{2-x}\text{Sr}_x\text{CuO}_4$ to look for evidence of local LTT symmetry tilts. We chose to study the Sr doped, rather than the Ba doped, systems since ionic size effect disorder is less in this system. This is due to the fact that Sr^{2+} is closer in size to La^{3+} than is Ba^{2+} . This means that the disorder introduced into the structure due to ionic size effects is minimal and any disorder in the local tilts will originate mainly from an inhomogeneous electronic charge distribution.

In this paper we show that the local octahedral tilt amplitude can be measured accurately using PDF techniques. If the tilt amplitude is large enough it is also possible to distinguish the tilt direction. We show that the local tilts are clearly LTO in nature in the undoped compound, as expected. However, away from zero doping ($x > 0$) the PDF is consistent with the presence of tilt disorder in the form of a mixture of tilt directions and a mixture of tilt amplitudes. As x increases at low temperature the local tilt amplitude decreases smoothly following the behavior of the average tilts. However, small but finite tilts persist locally when the sample goes into the high temperature tetragonal (HTT) phase above $x = 0.20$. In the Discussion section we present topological tilt models which qualitatively explain the origin of tilt disorder in the presence of charge stripes and show that the PDF data are well explained by a mixture of locally small and large amplitude tilts.

II. EXPERIMENT

Powder samples were prepared by conventional solid state reactions. Mixtures of La_2O_3 , SrCO_3 , and CuO were calcined at various temperatures between 900°C and 1050°C with several intermediate grindings. The products were sintered at 1100°C for 100 h, followed by an oxygen anneal at 800°C for 100 hours.

Time-of-flight neutron diffraction measurements were carried out on $\text{La}_{2-x}\text{Sr}_x\text{CuO}_4$ (LSCO) powder samples (approximately 10 g of each) for the range of doping ($0 \leq x \leq 0.30$) at 10 K temperature. Experiments were performed on the Special Environment Powder Diffractometer (SEPD) at the Intense Pulsed Neutron Source (IPNS) at Argonne National Laboratory.

The data were corrected for experimental effects and normalized³¹ to obtain the total scattering function $S(Q)$,²⁹ where $Q = |\mathbf{Q}| = |\mathbf{k} - \mathbf{k}_0|$ represents the momentum transfer magnitude for the scattering. The PDF function, $G(r)$, is then obtained by a Fourier transformation according to,

$$G(r) = \frac{2}{\pi} \int_0^\infty Q[S(Q) - 1] \sin(Qr) dQ. \quad (1)$$

The function $G(r)$ gives the probability of finding an atom at a distance r from another atom. This function is obtained directly from the Fourier transform of the neutron-diffraction data and is used to investigate features of the *local* structure of a material.³¹

Local structural information is obtained from the data by a process of modeling.³¹ A model structure is proposed and the PDF calculated. Parameters in the model are then varied to optimize the agreement between the calculated and measured PDFs. The procedure is similar to the traditional reciprocal-space based Rietveld method⁴⁷ for obtaining crystal structures from powder diffraction data; however, it is carried out in real-space and yields the local structure rather than the average crystal structure.³¹ From the refinements, different structural information can be extracted, such as lattice parameters, average atomic positions and amplitudes of their thermal motion, atomic displacements, and magnitudes of local octahedral tilts. The modeling procedure has been described in detail elsewhere.³¹

III. RESULTS

A. Local Tilt Amplitudes as a Function of Doping

Initially we investigate the appearance in the PDF of the octahedral tilts and show the extent to which the PDF technique can detect their presence. In Fig. 1(a), we compare three *model* PDFs to show qualitatively the effect of a change in the local octahedral tilt amplitude on $G(r)$. The PDFs are shown for the LTO structure with

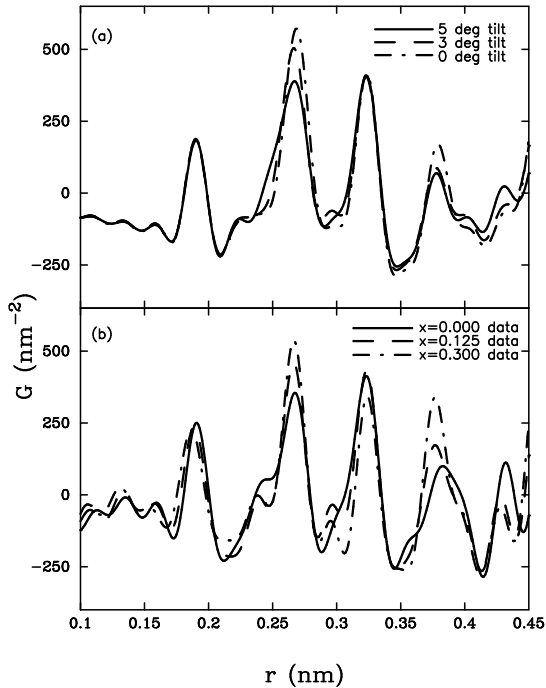


FIG. 1. (a) Comparison between three *model* PDFs. The models have LTO symmetry with 5° tilts (solid line), 3° tilts (dashed line), and 0° tilts (dash-dotted line). (b) Three different 10 K *data* PDFs that approximately correspond to the same tilt magnitudes as shown in the models in panel (a): $x = 0$ (solid line, $\approx 5^\circ$ tilt), $x = 0.125$ (dashed line, $\approx 3^\circ$ tilt), and $x = 0.30$ (dash-dotted line, $\approx 1^\circ$ tilt). The PDF technique clearly differentiates between the presence and absence of the tilts and these qualitative differences are evident in the data.

three different magnitudes of octahedral tilt: 0° (dash-dotted line), 3° (dashed line) and 5° (solid line). The initial parameters used in the models were obtained by converging the fit of the LTO model-PDF to the data-PDF from the $x = 0.125$ data-set at 10 K, using the RESPAR Real-Space Rietveld program.³¹ The octahedral tilt angles were then calculated independently from the positions of the in-plane oxygen (O1) and the out-of-plane oxygen (O2). These tilt angles are denoted by $|\theta_{O1}|$ and $|\theta_{O2}|$ respectively. The tilt angle $|\theta_{O1}|$ was obtained from the z -displacement of O1 using

$$|\theta_{O1}| = \left| \arctan \left(\frac{c \delta O1_z}{b \delta O1_y} \right) \right|, \quad (2)$$

where $\delta O1_z$ and $\delta O1_y$ are the z and y fractional coordinates respectively of O1, and c and b are the corresponding lattice parameters. Similarly, the average tilt is obtained from displacements of O2 using

$$|\theta_{O2}| = \left| \arctan \left(\frac{b \delta O2_y}{c \delta O2_z} \right) \right|. \quad (3)$$

In the case where the octahedral tilts are rigid, $|\theta_{O1}| = |\theta_{O2}|$. The tilt angles were then artificially adjusted to 5° , 3° and 0° in the model and the atomic positions for O1 and O2 determined from Eqs. 2 and 3. All other parameters in the model were held constant. In this way we could compare the effect of a change in tilt magnitude on the PDF neglecting other changes such as changes in bond-length or lattice parameter. As expected, the Cu-O nearest neighbor peak at 1.89 \AA is unaffected (the tilts are essentially rigid) but the peak at 2.7 \AA , which contains the La-O1 and La-O2 correlations (as well as the O1-O1 correlations), shows a particularly large change.

The lower panel, Fig. 1(b), presents PDFs obtained from the experimental data: $x = 0$ doping (solid line), where tilts of approximately 5° are present, $x = 0.125$ doping (dashed line) with tilts of approximately 3° , and $x = 0.30$ doping (dash-dotted line), with average tilts of zero. The changes in the data with doping are large and qualitatively similar to those expected for reductions in local tilt amplitude. In addition, a shortening of the average Cu-O bond is evident by a shift to the left of the nearest neighbor Cu-O peak, as expected from the average structure. This also gives an indication of the sensitivity of $G(r)$ to small structural changes such as this lattice contraction.

We have determined quantitatively the amplitudes of the local octahedral tilts as a function of doping using the LTO model and the Real-Space Rietveld modeling program. Characteristic fits are shown in Fig. 2 for the undoped material (average tilts are large) and the overdoped material (average tilts are zero). Difference curves are plotted below the PDFs. The agreement of the HTT model to the $x = 0.3$ data is significantly poorer than the fit of the LTO model to the undoped material. As we discuss later, this is because small but finite local tilts are still present in the structure even in the HTT phase.

The local tilt angles obtained from the fits are shown in Fig. 3 plotted as a function of doping, shown as filled circles. For comparison, average tilt angles obtained from a crystallographic analysis⁴⁸ are also plotted (shown as open circles). There is excellent agreement for lower dopings. The agreement is less good for compositions above $x = 0.15$. In this region the long-range average tilt angle is constrained to be zero because of the change in the average symmetry accompanying the phase change from LTO to HTT. However, in the PDF a better fit to the data is obtained when the LTO model is used, rather than the HTT model, and a small but finite ($\approx 1 - 2^\circ$) local tilt is refined.⁴⁹ The use of the LTO model to describe the local structure, even when the global structure is clearly HTT, is justified since the broken symmetry phase may persist locally. However, this analysis does not imply that, in our samples, the global structure is LTO in this region of doping.

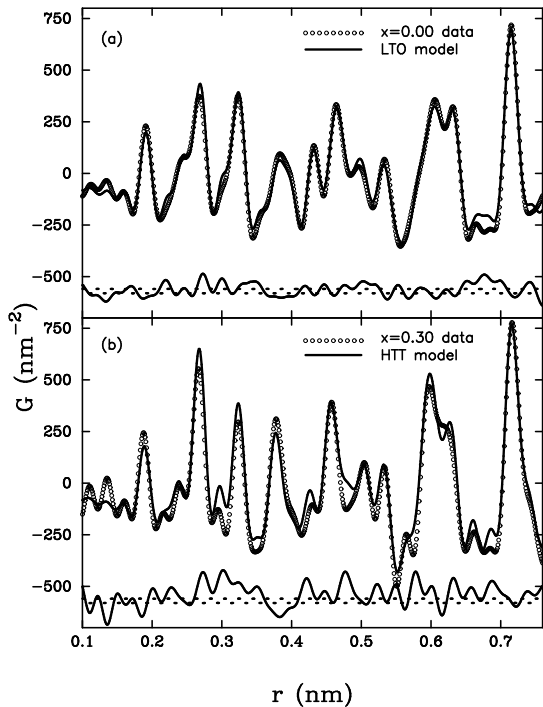


FIG. 2. (a) Fully converged PDF for the LTO model (solid line), and experimentally obtained PDF for LSCO with $x=0$ at 10 K (open circles). The difference curve is plotted below as a solid line. The dotted line shows the expected errors at the level of two standard deviations. (b) Fully converged PDF for the HTT model (solid line), and LSCO with $x=0.30$ at 10 K (open circles).

B. Local Tilt Directions as a Function of Doping

We would like to use the PDF technique to differentiate between local tilts with the [010] (LTO: tilt axis 45° rotated with respect to planar Cu-O bond) and [110] (LTT: tilt axis is parallel to the Cu-O bond) tilt symmetries since evidence for local LTT-like tilts might suggest the presence of charge stripes.

In Fig. 4 we show a comparison of two model PDFs, one where the tilts belong to the LTO type, and the other that is of LTT type. In Fig. 4(a) we show the difference for the case of a 5° tilt magnitude and in Fig. 4(b) for a smaller 3° tilt. It is important to emphasize that the only difference between our models is in the tilt symmetry (or directions of the tilts), keeping all other parameters constant, including tilt amplitude. Therefore, the difference in the PDFs that is shown is *only* due to the change in the tilt symmetry.

As is usual with the PDF, some regions of the function are much more strongly affected by the change than others. A change in tilt direction affects the peaks around 2.67 \AA and 2.95 \AA , that correspond to (La/Sr)-O1 and (La/Sr)-O2 bonds respectively. There is also a large effect on the peak located close to 6.0 \AA . Elsewhere in the

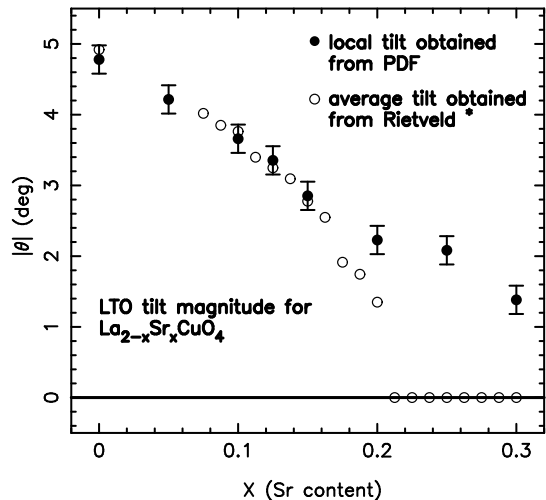


FIG. 3. Dependence of the local octahedral tilt angle magnitude (black circles), $|\theta|$, on Sr content, x . Open circles present average tilt angle magnitude obtained from Rietveld refinement done by Radaelli and collaborators (see text). The result shows that $|\theta|$ smoothly decreases when x is increased. However, significant local tilts persist even when the average tilts disappear. The data were collected at 10 K.

PDF the changes are small. Notice that the peaks at $\approx 2.8 \text{ \AA}$ give a characteristic “W-shaped” feature in the difference curve, while the peak at $\approx 6 \text{ \AA}$ gives a characteristic “M-shaped” feature. The changes are similar, but much smaller, as the local tilt amplitude diminishes.

In Fig. 5 we present fully converged fits of the LTO and LTT models to the undoped material. It is clear that the undoped material has local octahedral tilts that have the LTO symmetry: the fit is much better everywhere with the LTO model, and particularly large fluctuations are observed around $r = 2.8 \text{ \AA}$ in the LTT model.

We are interested if evidence for local LTT-like tilts appears as the CuO_2 planes are doped. In the set of Figures 5–8 we show the PDFs for samples with different dopings: again, upper panels show the PDF for fully converged LTO models (solid line) and experimental PDFs (open circles) with corresponding difference curves; lower panels compare PDFs for fully converged LTT models (solid line) with the PDFs obtained from the data (open circles), and give corresponding difference curves.

In Fig. 6, for $x = 0.05$ we again see that the LTO fit is better than the LTT one overall, and the characteristic *M*-feature is evident in panel (b). The underlying local tilts are still predominantly LTO-like.

For $x = 0.10$ the situation is less clear. The tilt amplitude is now down to 3.6° making differentiation between LTO and LTT harder. Both models fit quite well. However, we note that in the critical region around $r = 2.8 \text{ \AA}$ the LTT model actually has a *better* agreement with the data than the LTO model and in this case the difference curve from the LTO model has an *M*-shaped fluctuation

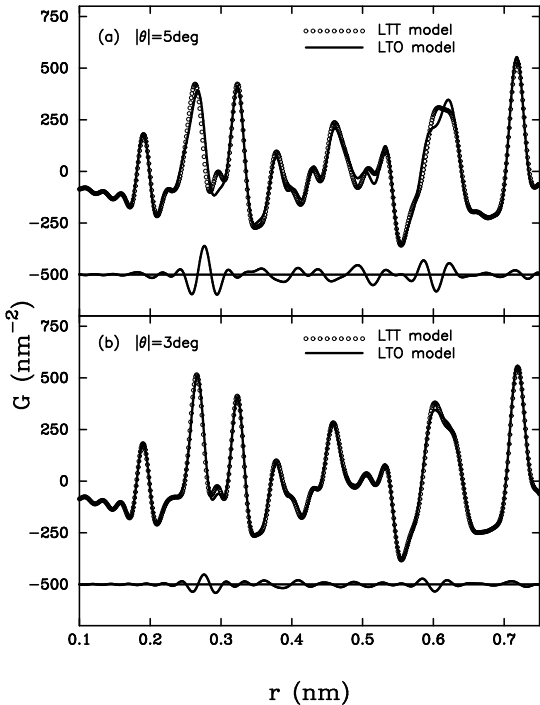


FIG. 4. Difference in model PDFs for the LTT and LTO tilt symmetry: (a) 5° case, and (b) 3° case. The PDF for the LTT model is given as a solid line, while that for the LTO model is presented with open circles. Difference curve is given below PDFs for both cases.

centered at $r = 2.8 \text{ \AA}$ consistent with some local LTT-like tilts.

As doping is raised beyond it becomes difficult to differentiate between the LTO and LTT models. Both models fit quite well as evidenced, for example, by the $x = 0.20$ data set shown in Fig. 8.

IV. DISCUSSION

A. Tilt magnitude vs. doping

The evolution of the *local* tilt magnitude, determined by fitting the LTO model to the PDFs from the data, decreases smoothly with increasing doping. This is consistent with crystallographic studies which show a smoothly decreasing *average* tilt amplitude with doping.^{48,50} Furthermore, it is clear from Fig. 3 that the average *local* tilt amplitude is quantitatively the same as the long-range ordered average tilt. Although this may not seem surprising, it is widely observed in these materials that the average *local* tilt amplitude can deviate significantly from the long-range ordered value. This occurs when finite local tilts exist but the tilt directions become disordered and the long-range tilt order is not preserved. This is very similar to a ferromagnetic-paramagnetic tran-

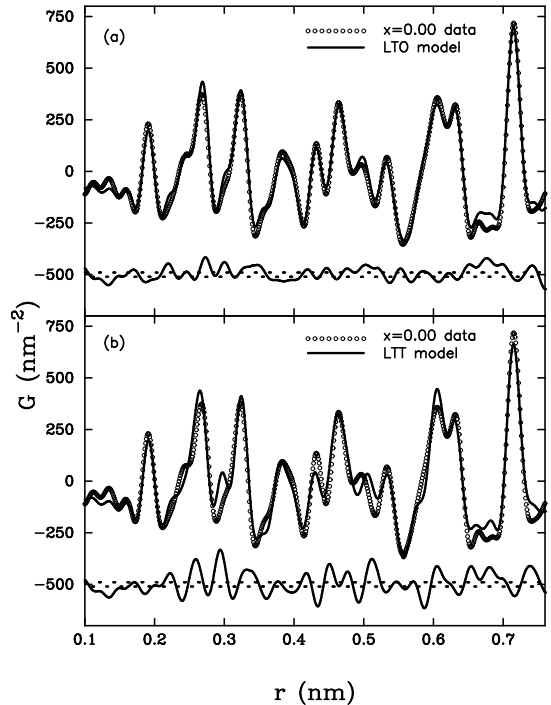


FIG. 5. (a) Fully converged model PDF with the LTO tilt symmetry (solid line) compared to experimental PDF for $x=0$ at 10 K (open circles). Difference curve is shown below the PDFs as a solid line. The dotted line shows the expected errors at the level of two standard deviations. (b) The same for the case of LTT tilt symmetry.

sition where the local moment survives but the long-range ordered moments average to zero. This behavior is seen in the temperature dependence of the tilts in these systems.^{41–43,51,52} The present result shows that the real, local, tilt is decreasing as x increases: in these materials the tilts are not just becoming disordered at low temperature by the action of doping but are smoothly decreasing.

This is easy to understand by the argument that the copper-oxygen bond is shortening as holes are doped and this anti-bonding bond is stabilized. The plane buckling occurs because the CuO_2 planes are constrained to fit continuously with the rare-earth oxide charge reservoir layers.⁵³ The buckling allows them to maintain a continuous structure with the charge reservoir layers while relieving stress introduced because the Cu-O bonds are just too long to fit perfectly. As the Cu-O bonds are shortened by doping the amplitude of tilt needed to relieve this stress is reduced and the tilts smoothly decrease.

In the high-doped region there is not perfect agreement between the local and long-range ordered tilt amplitudes. The crystallographic result is constrained to be zero above $x = 0.2$ where the global structure goes to the HTT phase. There is a remanent amount of tilting of around $1\text{-}2^\circ$ which persists even into the HTT phase. This is not completely unexpected because of the pres-

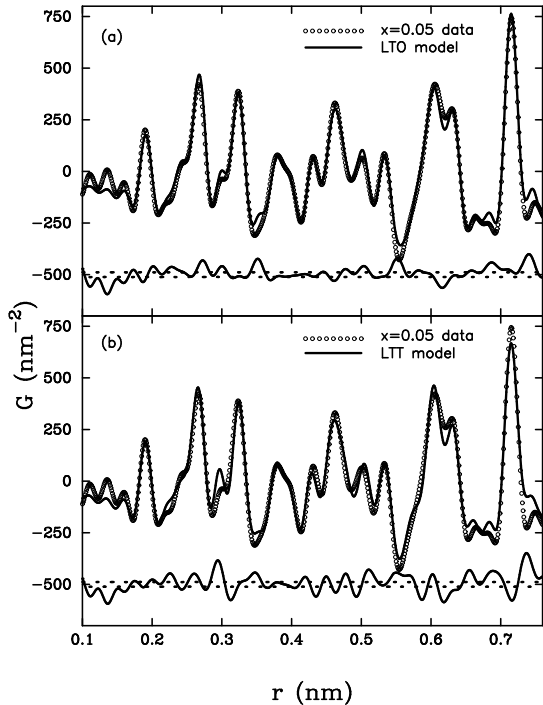


FIG. 6. (a) Fully converged model PDF with the LTO tilt symmetry (solid line) compared to experimental PDF for $x=0.05$ at 10 K (open circles). The difference curve is shown below the PDFs as a solid line. The dotted line shows the expected errors at the level of two standard deviations. (b) The same for the case of LTT tilt symmetry.

ence of Sr impurities in the structure which would be expected to modify the octahedral tilting in their immediate vicinity.^{11,43} It does not necessarily imply any significance with respect to the charge doping in the planes themselves.

B. Tilt direction vs. doping

If charge is doped into the material, it can be either distributed uniformly or it can be localized and over some doping range it can form charge stripes. Localized charge would cause local polaronic distortions, forcing the octahedra to change their shape, and affecting the magnitude of the tilts in the vicinity of the polaron. In addition, the presence of charge stripes should affect the direction of the octahedral tilting since it has been observed that long-range ordered charge stripes in the 2:1:4 materials have only been seen in samples in the LTT phase. Thus, the observation of *local* LTT-like tilts would be evidence for the presence of *local* charge-stripe order.

Local LTT-like tilts have been seen in the LTO phase of $\text{La}_{1.875}\text{Ba}_{0.125}\text{CuO}_4$.³⁹ In this case tilt amplitude is larger than it is in the Sr doped case reported here (3.8° for Ba,⁵¹ $x=0.15$, vs 2.9° for Sr, $x=0.15$, both at 10 K)

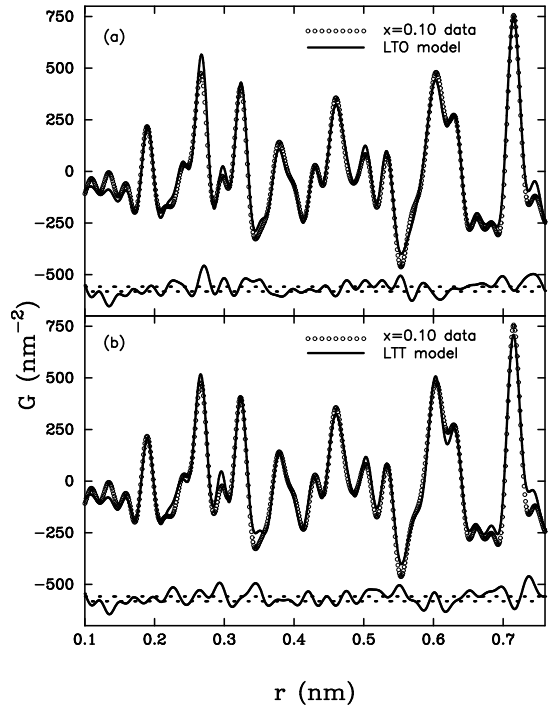


FIG. 7. (a) Fully converged model PDF with the LTO tilt symmetry (solid line) compared to experimental PDF for $x=0.10$ at 10 K (open circles). The difference curve is shown below the PDFs as a solid line. The dotted line shows the expected errors at the level of two standard deviations. (b) The same for the case of LTT tilt symmetry.

which explains why it was more clearly evident in the Ba doped case. At the time, there was no obvious physical justification for the presence of local LTT-domains which were globally disordered. However, it could be explained if the local LTT-like tilts are stabilized by the presence of local charge stripe order and if the charges are fluctuating dynamically. Long-range LTT tilt order would also be inhibited at doping fractions away from rational numbers where the holes can order commensurately with the lattice, even if the tilts were locally LTT-like. Models proposed in the earlier work showed that global LTO symmetry can be recovered by a linear superposition of two degenerate local LTT variants. Thus, spatially or temporally fluctuating LTT domains can yield a global LTO tilt symmetry.

The picture of local, fluctuating, LTT-like domains is also consistent with recent thermal conductivity measurements¹⁴ where the apparently contradictory result was obtained that the thermal conductivity (κ) of insulating samples of rare-earth doped $\text{La}_{2-x}\text{Sr}_x\text{CuO}_4$ was *higher* than that of similar samples which were conducting. Clearly the contribution of the charge carriers to the thermal transport is negligible, which is not surprising because of the low carrier density; but also implied by this result is that the inelastic phonon scattering is sig-

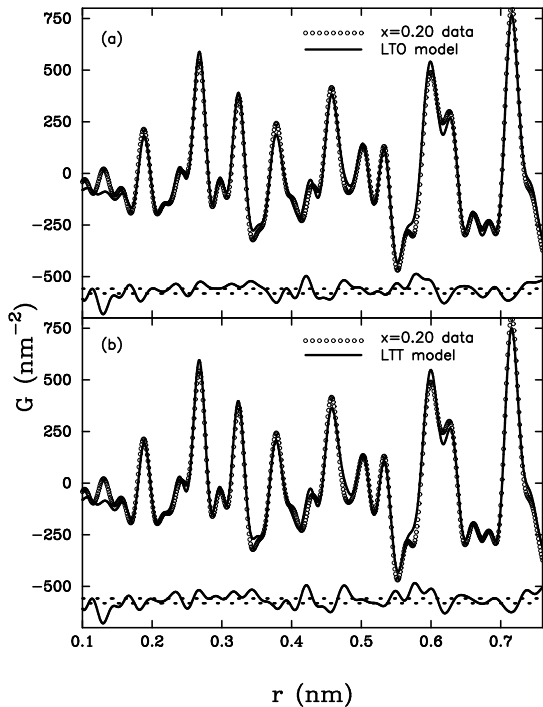


FIG. 8. (a) Fully converged model PDF with the LTO tilt symmetry (solid line) compared to experimental PDF for $x=0.20$ at 10 K (open circles). The difference curve is shown below the PDFs as a solid line. The dotted line shows the expected errors at the level of two standard deviations. (b) The same for the case of LTT tilt symmetry.

nificantly greater in metallic samples than in insulating ones. The authors proposed that scattering was occurring off local domains of stripes. We would like to add that, in the present picture, this phonon scattering would be greatly enhanced if there were fluctuating domains of *tilt* disorder associated with these striped domains. The result that there are regions of locally fluctuating LTT tilts is also consistent with measurements of the anelastic spectra from $\text{La}_2\text{CuO}_{4+\delta}$ ⁵⁴ which indicate elastic relaxations consistent with octahedral tilts tunneling between different LTT domains.

The first result we have demonstrated here is that the local tilt direction in undoped La_2CuO_4 is [010] (LTO), and that the PDF is clearly sensitive to the tilt direction for tilts of magnitude $\approx 5^\circ$. The local tilt direction and magnitude is the same as the average crystallographic tilt direction and magnitude for the undoped material at low temperature and there is no tilt disorder.^{48,50}

For doping levels greater than zero the PDF results are suggestive of the presence of local LTT-like tilts. The tilt directions and magnitudes are disordered, and also could be fluctuating and could originate from an inhomogeneous charge distribution in the CuO_2 planes. As we discuss below, we expect that charge localization in a background of octahedral tilts will give rise to complex

patterns of tilt disorder which our simplistic modeling using pure LTO and LTT models cannot hope to reproduce. Below we describe qualitatively different models of tilt defects which give insight as to when LTO and LTT tilts, respectively, are stabilized.

C. Tilt Defect Models

We introduce here several different models for the tilt distortions which might be expected as a result of the presence of localized charges in the tilt background. Our starting point is based on the two following observations: (a) Buckling appears because Cu-O bonds are too long to match the bonding in the La-O intergrowth layers,⁵³ and (b) Cu-O bonds become shorter on doping.

In the absence of holes the equilibrium tilt amplitude is 5° . On average, the tilts disappear for $x \approx 0.2$ which corresponds to a nominal copper charge-state of $+2.2$. If charges completely localize, the charge state of the copper is $+3$ which is easily high enough to remove the local tilt. However, between the localized charges the material is essentially undoped and large tilts are expected. Because the CuO_2 planes are a continuous network of corner shared octahedra, these untilted defects will introduce strains and there is expected to be a distribution of tilt amplitudes. However, it is possible to show geometrically that local LTT tilted octahedra (LTT-defects) can help reduce the strains.

We make the following assumptions in our models. First, the undistorted tilt pattern is LTO-like. Second, that the localized doped holes form into stripes with one hole associated with every second CuO_6 octahedron along the stripe.⁵ The nominal doping then determines the average separation of neighboring stripes. We then considered two possibilities. The first is that the charge essentially delocalizes along the chain making the Cu-O bonds along the chain short, but not shortening the Cu-O bonds perpendicular to the stripe. The second is that each charge localizes on a single CuO_6 octahedron, similar to a Zhang-Rice singlet,⁵⁵ sharing charge density equally between each of the four in-plane Cu-O bonds. We introduce these defects into the background of LTO tilts with the constraint that the octahedra are corner shared and displacements of an oxygen ion must be the same for neighboring octahedra. This gives rise to extended defects which we can identify using only these topological constraints. We will refer to the first case as Model I and the second case as Model II. Both models were made for the case of $x = 0.125$ doping.

1. Model I

With the LTO tilts, all of the O1 ions are displaced out of the plane, either up or down. By shortening two of the in-plane bonds along the direction of the charge

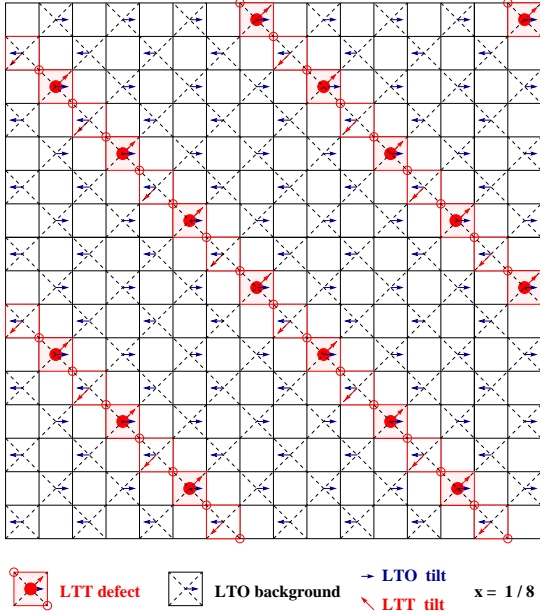


FIG. 9. Schematic view of the Model I (see text) tilt pattern in the CuO_2 plane in the presence of charge stripes. Corner shared CuO_6 octahedra are denoted by squares with dashed crosses inside. The displacement of the apical oxygen above the plane due to octahedral tilting is shown with small arrows. In-plane O1 ions lie at the corners of the octahedra and are displaced up or down by the tilts (not shown). Open circles at the corners indicates an O1 ion which is undisplaced and lies in the plane. The presence of a localized hole is indicated by a black circle.

stripe we expect this to bring the two O1 ions which lie along the stripe (denoted by open circles in Fig. 9) into the plane from their displaced positions. The bonds perpendicular to the stripe remain long. In this case, the local tilt persists, but changes from LTO-like to LTT-like in the stripe. The LTO tilt pattern between the stripes is preserved, though the amplitude of the LTO tilts may be locally distorted where it joins the LTT-stripes.

From Fig. 9, for $\frac{1}{8}$ doping we expect to get a ratio of LTT:LTO tilted octahedra of 2:6. This number is given by the ratio of the width of the stripe to the width of the undoped domain; in this case 1:3. In general, for $\frac{1}{n}$ holes per copper this ratio is given by $1: \frac{n-2}{2}$.

This model predicts that in the presence of charge stripes the local tilt distribution should be a mixture of LTO and LTT tilts with a majority of LTO tilts in the doping range up to $x = 0.25$.

2. Model II

In this model the localized holes on every second site along the stripe produce octahedra which are completely untilted. This is equivalent to placing an HTT defect in

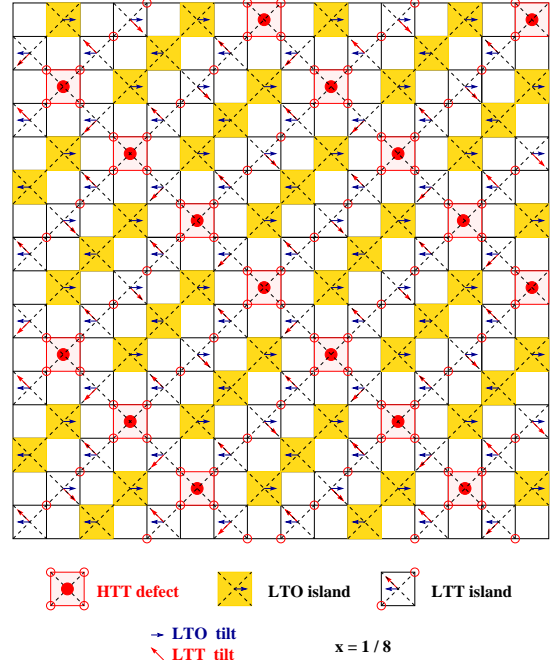


FIG. 10. Schematic view of the Model II (see text) tilt pattern in the CuO_2 plane in the presence of charge stripes. Corner shared CuO_6 octahedra are denoted by squares with dashed crosses inside. The displacement of the apical oxygen above the plane due to octahedral tilting is shown with small arrows. In-plane O1 ions lie at the corners of the octahedra and are displaced up or down by the tilts (not shown). Open circles at the corners indicates an O1 ion which is undisplaced and lies in the plane. The presence of a localized hole is indicated by a black circle at the center of the octahedron.

the LTO background. Because the out-of-plane displacements of the O1 ions are removed, neighboring octahedra both along the direction of the stripe, and perpendicular to the stripe, take on an LTT-like tilt, as shown in Fig. 10. The tilt axes of the LTT-like tilts propagating parallel and perpendicular to the stripes are rotated by 90° with respect to each other. As we pointed out in our earlier paper,³⁹ the linear superposition of these two degenerate LTT-variants yields the LTO symmetry of tilts on average.

As is clear from Fig. 10, patches of LTO-like tilts also persist in this model; however, the extent of the LTT-like tilting is greater than in Model I. In the case of $x = \frac{1}{8}$ the ratio of HTT:LTT:LTO is 1:4:3. In general, for $\frac{1}{n}$ holes the ratio will be

$$1 : \frac{n}{2} : \frac{n-2}{2}. \quad (4)$$

One assumption inherent in this model is that the LTT-stripes propagating perpendicular to the charge-stripes persist all the way to the neighboring stripe. This is an approximation since the Cu-O bonds are long along this stripe and O1 ion displacements may not completely

disappear along the stripe (even though these ions are depicted as open circles in Fig. 10). Thus, when the charge-stripes are well separated at low doping we might expect that the ratio of LTT:LTO is smaller than predicted by Eq. 4.

3. Discussion

These tilt models show that, if charge stripes are present, the real situation will be a mixture of LTO and LTT; or LTO, LTT and HTT tilts, and not purely LTO or LTT as we have modeled. The presence of charged stripes, and regions between the stripes with no holes present, implies that there coexists in the local structure regions with strongly diminished tilts, and regions with large tilts (as much as 5°) even in the doped materials whose average tilt is 3° or less. We would like to see whether this picture is consistent with our PDF data. We have made a simple test of this idea, and the results are shown in Fig. 11. In this figure we compare PDFs which mimic the situation we would have if there were a coexistence of 5° tilts and $\approx 2^\circ$ tilts, with the data from the $x = 0.10$ sample whose average tilt is 3.6° . We did this by averaging the data-PDFs from the $x = 0$ and $x = 0.25$ samples. The former has 5° LTO tilts and the latter sample has tilts with less than 2° of tilt amplitude. It is clear from the figure that the incoherent mixture of large and small tilts reproduces the data from the $x = 0.10$ sample excellently. For comparison, the data-PDFs from the $x = 0$ and $x = 0.25$ data are reproduced in the lower panel of this figure. There are large differences between them, yet when they are mixed together they give an excellent account of the $x = 0.10$ data. This shows that the data-PDFs for intermediate dopings are consistent with the presence of a distribution of local tilt magnitudes. Interestingly, the largest fluctuations in the difference curve between the $x = 0.10$ data and the mixture occur at $r \approx 2.8 \text{ \AA}$ and $r \approx 6 \text{ \AA}$ which is exactly where fluctuations are expected if local LTT-like tilts are present. This is also consistent with the fact that an inhomogeneous local tilt distribution exists in this material. These results are consistent with the observations of Hammel et al.^{11,13,44,56} of an inhomogeneous tilt distribution in doped $\text{La}_{2-x}\text{Sr}_x\text{CuO}_4$ and $\text{La}_2\text{CuO}_{4+\delta}$ from NMR measurements. These authors measure the electric field gradient at the La site which is very sensitive to local tilt disorder and find a continuous distribution of La environments similar to what would be expected from our models if local strains were also present. We cannot compare quantitatively the tilt amplitudes because there is not a direct relationship between EFG and octahedral tilt angle. The octahedral tilt angle can be found from point-charge models, or more accurately from quantum cluster calculations⁵⁶; however, these authors have not published values for the tilt amplitudes. Nonetheless, there is excellent qualitative agreement.

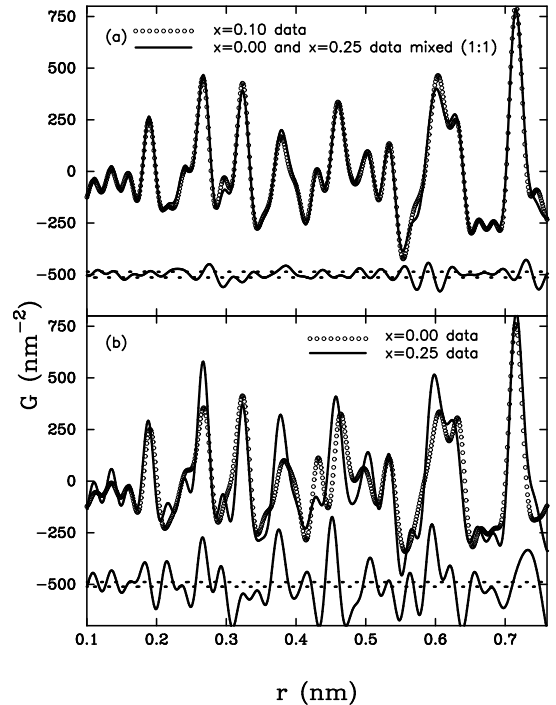


FIG. 11. (a) Comparison of PDFs produced by a mixture of large and small tilt amplitudes and the data from the $x = 0.10$ sample. The solid line is the PDF obtained by mixing the $x = 0$ data set (5° tilts) with the $x = 0.25$ ($< 2^\circ$ tilts) data set in the ratio 1:1 to mimic the effect of a coexistence of large and small tilts in the local structure. The open circles show the PDF from the the $x = 0.10$ sample. (b) The $x = 0$ and $x = 0.25$ data-PDFs are plotted for comparison. There are large differences between these PDFs, yet when they are mixed they reproduce the PDF of the intermediate composition extremely well. The data were collected at 10 K.

V. CONCLUSIONS

In conclusion, we have shown that the PDF technique clearly differentiates between the presence and the absence of local tilts of CuO_6 octahedra. The magnitude of the local octahedral tilts in $\text{La}_{2-x}\text{Sr}_x\text{CuO}_4$ smoothly decreases as a function of Sr-content at $T=10 \text{ K}$. This result is in agreement with the result for the average tilt angle magnitude,^{48,50} obtained using standard crystallographic methods. Small but significant local tilts persist above $x = 0.20$ in the HTT structural phase where the tilts are not allowed crystallographically.

We showed that the PDF technique can differentiate between different tilt directions, providing their magnitude is large enough. Our analysis showed that for the undoped material the local tilts clearly have the LTO symmetry, in agreement with crystallography, indicating that there is no tilt disorder at this composition. For $x = 0.05$, the local tilts are still predominantly LTO-like. As doping is increased, there is some evidence that LTT-like tilts might be present, but in the interesting su-

perconducting region of the phase diagram the tilt amplitudes are small enough that the PDF is at the limit of its sensitivity.

We have presented topological models for the tilt disorder we expect to be present in these materials in the presence of charge-stripes. These imply that if charge stripe domains exist locally there should be a coexistence of large and small tilts, and LTO and LTT-like tilts locally. A simple test using PDF data shows that this is consistent with our measured PDFs. A single crystal diffuse scattering, or electron diffraction measurement may be useful for elucidating this point.

ACKNOWLEDGMENTS

We are grateful to T. Egami, D. Haskel, D. Louca, R. McQueeney, E.A. Stern and J.D. Thompson for stimulating discussions. The work at Michigan State University was supported financially by NSF through grant DMR-9700966. SJB is a Sloan Research Fellow of the Alfred P. Sloan Foundation. The work at Los Alamos was done under the auspices of the Department of Energy, under the contract W-7405-ENG-36. The experimental data were collected on the SEPD diffractometer at the IPNS at the Argonne National Laboratory. This facility is funded by the US Department of Energy under Contract W-31-109-ENG-38.

-
- ¹ J. M. Tranquada, D. J. Buttrey, V. Sachan, and J. E. Lorenzo, *Phys. Rev. Lett.* **73**, 1003 (1994).
- ² V. Sachan, D. J. Buttrey, J. M. Tranquada, J. E. Lorenzo, and G. Shirane, *Phys. Rev. B* **51**, 12742 (1995).
- ³ A. Vigliante, M. von Zimmermann, J. R. Schneider, T. Frello, N. H. Andersen, D. J. B. J. Madsen, D. Gibbs, and J. M. Tranquada, *Phys. Rev. B* **56**, 8248 (1997).
- ⁴ J. M. Tranquada, P. Wochner, and D. J. Buttrey, *Phys. Rev. Lett.* **79**, 2133 (1997).
- ⁵ J. M. Tranquada, B. J. Sternlieb, J. D. Axe, Y. Nakamura, and S. Uchida, *Nature* **375**, 561 (1995).
- ⁶ J. M. Tranquada, J. D. Axe, N. Ichikawa, Y. Nakamura, S. Uchida, and B. Nachumi, *Phys. Rev. B* **54**, 7489 (1996).
- ⁷ M. von Zimmermann, A. Vigliante, T. Niemöller, N. Ichikawa, T. Frello, J. Madsen, P. Wochner, S. Uchida, N. H. Andersen, J. M. Tranquada, D. Gibbs, and J. R. Schneider, *Europhys. Lett.* **41**, 629 (1998).
- ⁸ C. H. Chen and S-W. Cheong, *Phys. Rev. Lett.* **76**, 4042 (1996).
- ⁹ C. H. Chen, S-W. Cheong, and H. Y. Hwang, *J. Appl. Phys.* **81**, 4326 (1997).
- ¹⁰ A. P. Ramirez, P. Schiffer, S-W. Cheong, C. H. Chen, W. Bao, T. T. M. Palstra, P. L. Gammel, D. J. Bishop, and B. Zegarski, *Phys. Rev. Lett.* **76**, 3188 (1996).
- ¹¹ P. C. Hammel, B. W. Statt, R. L. Martin, F. C. Chou, D. C. Johnston, and S-W. Cheong, *Phys. Rev. B* **57**, R712 (1998).
- ¹² T. Egami, D. Louca, and R. J. McQueeney, *J. Supercond.* **10**, 323 (1997).
- ¹³ B. W. Statt, P. C. Hammel, Z. Fisk, S-W. Cheong, F. C. Chou, D. C. Johnston, and J. E. Schirber, *Phys. Rev. B* **52**, 15 575 (1995).
- ¹⁴ O. Baberski, A. Lang, O. Maldonado, M. Hücker, B. Büchner, and A. Freimuth, LANL preprint archive, cond-mat/9712136, 1997.
- ¹⁵ V. J. Emery, S. A. Kivelson, and O. Zachar, *Phys. Rev. B* **56**, 6120 (1997).
- ¹⁶ M. I. Salkola, V. J. Emery, and S. A. Kivelson, *Phys. Rev. Lett.* **77**, 155 (1996).
- ¹⁷ Yu. A. Krotov, D-H. Lee, and A. V. Balatsky, *Phys. Rev. B* **56**, 8367 (1997).
- ¹⁸ R. S. Markiewicz, unpublished.
- ¹⁹ J. C. Phillips, *P. Natl. Acad. Sci. USA* **94**, 12771 (1997).
- ²⁰ A. Bianconi, A. Valletta, A. Perali, and N. L. Saini, *Solid State Commun.* **102**, 369 (1997).
- ²¹ T. Egami and S. J. L. Billinge, in *Physical Properties of High-Temperature Superconductors V*, edited by D. M. Ginsberg, Singapore, 1996, World-Scientific.
- ²² T. Egami and S. J. L. Billinge, *Progr. in Materials Science* **38**, 359 (1994).
- ²³ E. Salje, A. S. Alexandrov, and W. Y. Liang, editors, *Polarons and Bipolarons in High-T_c Superconductors and Related Materials*, Cambridge, 1995, Cambridge University Press.
- ²⁴ K. A. Müller and G. Benedek, editors, *Phase Separation in Cuprate Superconductors*, World Scientific, Singapore, 1993.
- ²⁵ E. Sigmund and K. A. Müller, editors, *Phase Separation in Cuprate Superconductors*, Springer-Verlag, New York, 1994.
- ²⁶ Y. Bar-Yam, T. Egami, J. Mustre-de Leon, and A. R. Bishop, editors, *Lattice Effects in High-Temperature Superconductors*, World Scientific, 1992.
- ²⁷ J. M. Tranquada, J. D. Axe, N. Ichikawa, A. R. Moodenbaugh, Y. Nakamura, and S. Uchida, *Phys. Rev. Lett.* **78**, 338 (1997).
- ²⁸ N. L. Saini, A. Lanzara, H. Oyanagi, H. Yamaguchi, K. Oka, T. Ito, and A. Bianconi, *Phys. Rev. B* **55**, 12759 (1997).
- ²⁹ B. E. Warren, *X-ray Diffraction*, Dover, New York, 1990.
- ³⁰ T. Egami, *Mater. Trans.* **31**, 163 (1990).
- ³¹ S. J. L. Billinge, in *Local Structure from Diffraction*, edited by S. J. L. Billinge and M. F. Thorpe, page 137, New York, 1998, Plenum.
- ³² J. D. Axe, A. H. Moudden, D. Hohlwein, D. E. Cox, K. M. Mohanty, A. R. Moodenbaugh, and Y. Xu, *Phys. Rev. Lett.* **62**, 2751 (1989).
- ³³ M. K. Crawford, R. L. Harlow, E. M. McCarron, W. E. Farneth, J. D. Axe, H. Chou, and Q. Huang, *Phys. Rev. B* **44**, 7749 (1991).
- ³⁴ B. Büchner, M. Breuer, W. Schlabitz, A. Viack, W. Schäfer, A. Freimuth, and A. P. Kampf, *Physica C* **235-240**, 281 (1994).
- ³⁵ B. Büchner, M. Breuer, A. Freimuth, and A. P. Kampf,

- Phys. Rev. Lett. **73**, 1841 (1994).
- ³⁶ S. J. L. Billinge, G. H. Kwei, A. C. Lawson, J. D. Thompson, and H. Takagi, Phys. Rev. Lett. **71**, 1903 (1993).
- ³⁷ D. E. Cox et al., Mater. Res. Soc. Symp. Proc. **156**, 141 (1989).
- ³⁸ K. Yvon and M. Francois, Z. Phys. B **76**, 413 (1989).
- ³⁹ S. J. L. Billinge, G. H. Kwei, and H. Takagi, Phys. Rev. Lett. **72**, 2282 (1994).
- ⁴⁰ T. Egami, W. Dmowski, J. D. Jorgensen, D. G. Hinks, D. W. Capone, III, C. U. Segre, and K. Zhang, Rev. Solid State Sci. **1**, 247 (1987).
- ⁴¹ S. J. L. Billinge and G. H. Kwei, J. Phys. Chem. Solids **57**, 1457 (1996).
- ⁴² D. Haskel, E. A. Stern, D. G. Hinks, A. W. Mitchell, J. D. Jorgensen, and J. I. Budnick, Phys. Rev. Lett. **76**, 439 (1996).
- ⁴³ D. Haskel, E. A. Stern, D. G. Hinks, A. W. Mitchell, and J. D. Jorgensen, Phys. Rev. B **56**, R521 (1997).
- ⁴⁴ P. C. Hammel, A. P. Reyes, S-W. Cheong, Z. Fisk, and J. E. Schirber, Phys. Rev. Lett. **71**, 440 (1993).
- ⁴⁵ R. S. Markiewicz, Physica C **193**, 323 (1992); R. S. Markiewicz, Physica C **217**, 381 (1993); R. S. Markiewicz, Physica C **210**, 235 (1993).
- ⁴⁶ R. S. Markiewicz, J. Phys. Chem. Solids **58**, 1179 (1997).
- ⁴⁷ H. M. Rietveld, J. Appl. Crystallogr. **2**, 65 (1969).
- ⁴⁸ P. G. Radaelli, D. G. Hinks, A. W. Mitchell, B. A. Hunter, J. L. Wagner, B. Dabrowski, K. G. Vandervoort, H. K. Viswanathan, and J. D. Jorgensen, Phys. Rev. B **49**, 4163 (1994).
- ⁴⁹ For example, the agreement factor, which is similar to the profile-weighted residuals function in Rietveld refinement³¹, equals 0.194 for the LTO model and 0.208 for the HTT model for the $x = 0.30$ data set, where the LTO model has 13 independent variables and the HTT model has 11 independent variables.
- ⁵⁰ M. Braden, P. Schweiss, G. Heger, W. Reichardt, Z. Fisk, K. Gamayunov, I. Tanaka, and H. Kojima, Physica C **223**, 396 (1994).
- ⁵¹ E. S. Božin, S. J. L. Billinge, and G. H. Kwei, Physica B **241-243**, 795 (1998).
- ⁵² E. S. Božin, S. J. L. Billinge, G. H. Kwei, and H. Takagi, unpublished, 1998.
- ⁵³ J. Zhou and J. B. Goodenough, Phys. Rev. B **56**, 6288 (1997).
- ⁵⁴ F. Cordero, C. R. Grandini, C. Cannelli, R. Cantelli, F. Trequattrini, and M. Ferretti, Phys. Rev. B **57**, 8580 (1998).
- ⁵⁵ F. C. Zhang and T. M. Rice, Phys. Rev. B **37**, 3759 (1988).
- ⁵⁶ R. L. Martin, Phys. Rev. Lett. **75**, 744 (1995).